The International Journal of Advanced Manufacturing Technology (2019) 102:4047–4058
https://doi.org/10.1007/s00170-019-03530-7

ORIGINAL ARTICLE

Optimization of SPS processing parameters on the density and hardness properties of graphene reinforced polylactic acid nanocomposite

O. T. Adesina[1] · E. R. Sadiku[2] · T. Jamiru[1] · O. F. Ogunbiyi[1] · L. W. Beneke[1] · A. T. Adegbola[1]

Received: 29 December 2018 / Accepted: 25 February 2019 / Published online: 5 March 2019

Abstract
This article examines the influence of process parameters of Spark plasma sintering (SPS) technique on the densification and hardness properties of graphene (GNP) reinforced polylactic acid (PLA) nanocomposite. The numerical experiment was designed in accordance with response surface methodology (RSM) using central composite design (CCD). Five percent GNP were used as reinforcement in the polylactic acid matrix at varying conditions of temperature and pressure for the physical experiment. The validation of the developed model, as well as the effect of each variable and their interaction, was analyzed using the analysis of variance (ANOVA). Taking the material hardness and density as the response of the designed experiment, the data obtained from both the numerical and physical experiment were statistically analyzed to obtain a predictive model which correlates the hardness and density as a function of the independent process parameters. The optimization produced 30 feasible solutions whose desirability equals to 1. The most desirable SPS processing parameters were the temperature of 158.2 °C and a pressure of 25.87 MPa. Under this condition, a density of 1.28 g/cm^3 and Vickers hardness value of 260.

Keywords Optimization · ANOVA · Polylactic acid (PLA) · Graphene (GNP) · Density · Hardness · Temperature · Pressure

1 Introduction

The development of eco-friendly and sustainable material has become a major area of research focus both in the industry and the academia to address issues of environmental concern. The use of bio-based or biodegradable and renewable material is being considered as a possible alternative to non-biodegradable petroleum-based material. According to a prediction made, by 2010, the production of plastics per year is expected to have risen to over 300 million tons [1]. This consumes a large amount of petroleum and results to the great release of CO_2 adversely affecting the health for the populace. Polylactic acid (PLA) is a renewable, sustainable, biodegradable, and eco-friendly thermoplastic polyester having balanced properties of mechanical strength, thermal plasticity, and composability for short-term commodity application [2–4]. It is prepared by ring polymerization of the lactic acid monomer and obtained via the fermentation of agricultural products such as corn and sugar beets. It has comparable attractive mechanical properties with petroleum-based polyolefin suitable for short-term application such as packaging, disposable sensors, and tissue engineering [5]. However, the mechanical and thermal properties of PLA have to be enhanced for its suitability for the long-term high-performance application. The effectiveness of nanofillers such as clay, carbon nanotube [6–8], and graphene [5, 9] in PLA has been proven as reinforcement for its extended applications.

Graphene is produced from natural graphite which makes its cheaper as nanoreinforcement compared with other carbon-based nanomaterial [10]. Graphene or graphite nanoplatelets (GNP) is a carbon nanomaterial composed of stacked 2D graphene sheet having mechanical strength (Young modulus of 1060 GPa), the electrical conductivity of approximately

✉ O. T. Adesina
oluwagbengaadesina@yahoo.com

[1] Department of Mechanical Engineering, Mechatronics, and Industrial Design, Tshwane University of Technology, Pretoria, South Africa

[2] Institute of NanoEngineering Research (INER) and Department of Chemical Metallurgy and Materials Engineering, Tshwane University of Technology, Pretoria, South Africa

Table 1 Experimental design and actual response results of density and hardness

Runs	Factors		Response 1	Response 2
	Temperature A (°C)	Pressure B (MPa)	Density (g/cm^3)	Hardness (HV)
1	160.00	30.00	1.288	265.00
2	135.00	30.00	1.282	243.31
3	129.82	25.00	1.276	230.76
4	147.50	17.93	1.283	249.55
5	135.00	20.00	1.278	235.94
6	147.50	25.00	1.284	251.61
7	147.50	32.07	1.287	255.16
8	147.50	25.00	1.284	251.61
9	147.50	25.00	1.284	251.61
10	147.50	25.00	1.284	251.61
11	165.18	25.00	1.288	264.44
12	147.50	25.00	1.284	251.61
13	160.00	20.00	1.285	257.42

10^4, and thermal stability [3]. Graphene, including GNPs, is often applauded as the next generation of nanofiller for polymers [11].

SPS technology operates via a pulsed electric current flowing directly through a compaction die and a powder sample in which a uniaxial load is applied. For an electrically insulated powder, indirect heating of the die is the only source of heating. The homogeneity in temperature distribution is obtained by optimization of the tools [12].

1.1 Previous studies on SPS of polymers

A very limited number of research on the consolidation of polymers using spark plasma sintering have been reported. The most prominently researched is polyamide [13–17]. It was reported that the applied pressure has a major influence on the mechanical properties of the sintered compact. Moreso, there is a level of dependence of suitable consolidation temperature on the applied pressure. At 200 °C, a pressure of 147 MPa was necessary to obtain a fully dense thermosetting PI sample and highest elastic modulus. Degradation occurs due to carbonization at a temperature above 300 °C at pressure > 19.6 MPa and at a temperature higher than 230 °C for a pressure of 39.2 MPa.

The possibility of processing any kind of thermoplastic and thermoset polymer was also presented in other few studies [12, 17–19].

PI-based composites were developed by Tanaka et al. [17] using SPS techniques for friction and wear applications. Polyimide (PI) was filled with carbon and diamond particles in order to improve the wear properties of the composites. The set pressure was 50 MPa and the sintering temperature of 220 °C. Above the sintering temperatures, some cracks were observed and the anti-wear properties were deteriorated.

Sebileau et al. [19] worked on the consolidation of polyetheretherketone by spark plasma sintering. The effect

Table 2 Analyses of variance (ANOVA) for response quadratic model of density of PLA/GNP composite using CCD

Source	Sum of squares	df	Mean square	F value	Prob. > F	
Model	1.42×10^{-4}	5	2.855×10^{-5}	86.10	< 0.0001	Significant
A-tempt	1.123×10^{-4}	1	1.12×10^{-4}	338.60	< 0.0001	
B-pressure	2.002×10^{-5}	1	2.002×10^{-5}	60.39	0.0001	
AB	2.500×10^{-7}	1	2.500×10^{-7}	0.75	0.4140	
A^2	7.853×10^{-6}	1	7.853×10^{-6}	23.68	0.0018	
B^2	1.33×10^{-6}	1	1.332×10^{-6}	4.02	0.0851	
Residual	2.321×10^{-6}	7	3.316×10^{-7}			
Lack of fit	2.321×10^{-6}	3	7.737×10^{-7}			
Pure error	0.000	4	0.000			
Cor. total	1.451×10^{-4}	12				

R^2, 0.9840; R^2 *adj*, 0.9726; *Adequate precision*, 30.359

Table 3 Statistical parameters of the model equation as obtained from ANOVA models for density

Type of variable	
Standard deviation (SD)	5.758×10^{-4}
Mean	1.28
Coefficient of variation C.V (%)	0.045
Prediction error sum of square (PRESS)	1.651×10^{-5}
R-squared	0.9840
Adjusted *R*-squared	0.9726
Pred *R*-squared	0.8862
Adequate precision	30.359

of SPS parameters such as temperature, pressure, and dwell time on density and the mechanical properties of PEEK were investigated using the design of experiments (DoE). The author also attributed the pressure as a significant parameter playing a positive or negative role on PEEK properties according to the responses obtained from the DoE studied. A temperature of 250 °C, a pressure of 40 MPa, and a dwell time of 20 min were identified as the optimal SPS process parameters.

Schwertz et al. [12] worked on the consolidation by spark plasma sintering of polyimide and polyetheretherketone. Dense polyimide and polyetheretherketone specimens were obtained at temperatures as low as 320 °C for PI and 200 °C for PEEK respectively. Relative densities above 99% were reached for both materials. Improved mechanical properties were obtained for compression and hardness test on the sintered samples.

Ge et al. [20] boosted the thermoelectric properties of PEDOT: PSS/inorganic nanoparticle composite using spark plasma sintering technique at 100 °C. The SPS prepared sample shows much better properties compare with the samples prepared by cold press technique. PEDOT: PSS with 33 wt.% $Cu_2S_nSe_3$ nanoparticle samples has the highest ZT value of 0.04 at 45 °C which is 20 times higher than the pristine

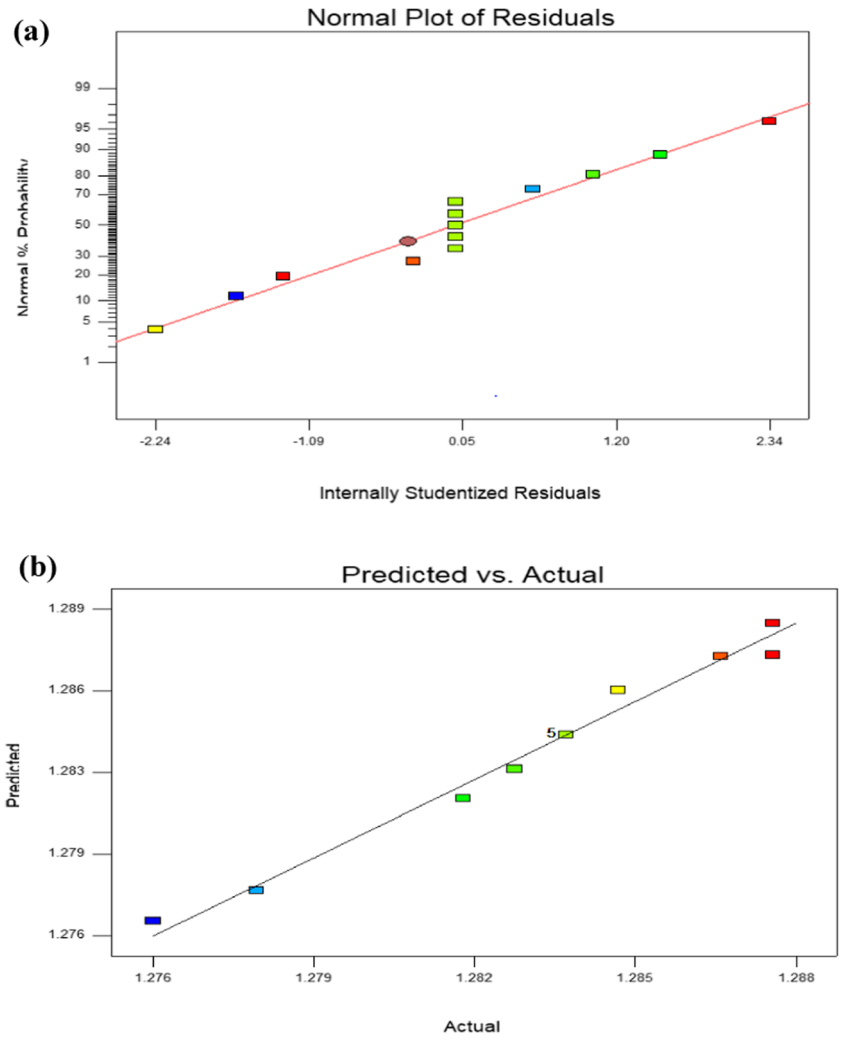

Fig. 1 Stochastic error and a deterministic portion for the density of PLA/GNP composites as normal probability plot for residuals (**a**) and predicted versus actual values (**b**)

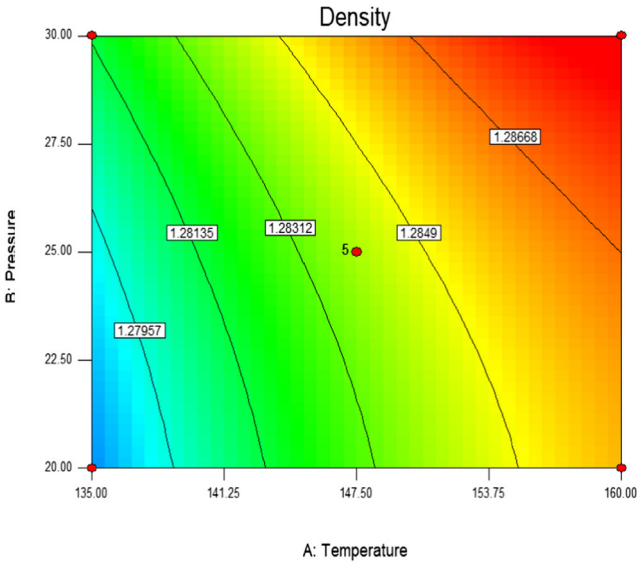

Fig. 2 Contour plot of density as a function of temperature and pressure

PEDOT—PSS bulk (0.02). Hence, SPS offers a new strategy to fabricate the polymer bulk material with boosted thermoelectric properties.

It was highlighted that the optimization of the SPS parameters and sufficient understanding of the SPS consolidation mechanism is needed. Although, the possibilities of using the SPS method in the consolidation of certain polymers were established in those researches findings. However, the feasibility of consolidating polylactic acid(PLA) and its nanocomposite has not been explored. Moreso, there is still limited research done on the PLA-based nanocomposite with graphene as reinforcement or nanofiller, hence the need for this study.

1.2 Recent studies on optimization of polylactic acid composite using RSM

Tharazi et al. [21] optimized the hot press parameters on the tensile strength property of unidirectional long kenaf fiber-reinforced polylactic acid composite using RSM and ANOVA. The experimental result shows that the three parameters examined which are; temperature, pressure, and heating time influenced the tensile strength property of the composite. The optimal tensile strength obtained was the combination of temperature, pressure, and time of 200 °C, pressure 3 MPa and 8 min respectively.

Shaari et al. [22] worked on the optimization of mechanical properties of silver nanoparticles(AgNPs)-loaded chitosan/polylactic acid. The analysis was performed by ANOVA and RSM. The concentration of Polyethylene glycol 400 (PEG) and the percentage volume (PLA/chitosan) were the factors considered while the responses were tensile strength and elongation. The optimal condition of 7.93% *w/w* of PEG, 28.79/71.2% of PLA/chitosan gave the optimal performance of 7.99 MPa and 32.6% elongation.

Ibrahim et al. [23] optimized the processing conditions of PLA nanocomposite using response surface methodology. Polylactide with a fixed amount (2% *w/w*) of organoclay Cloisite ® was melt intercalated. The process optimization was performed using response surface methodology. The processing temperature, rotor speed, and mixing time were chosen as the process parameters while the response was Young's modulus. The maximum Young modulus of 1211 MPa was obtained at temperature, speed, and time of 175 °C, 100 rpm, and 7 min respectively.

2 Physical experiment

2.1 Materials

PLA powder from Micro Powders, Inc., NY was used for the study. The density of 1.23–1.25 g/cm^3 was indicated by the supplier with a maximum particle size of 180 μm and a mesh size of 80. The melting point of PLA given by the supplier was 150–160 °C. Graphene nanoplatelets (GNP) was supplied by Sigma–Aldrich, having product code 900409. According to the product description, it is a new type of nanoparticle obtained from graphite. The GNP used in this experiment has an average diameter of 5 μm, an average thickness of 15 nm, and a typical surface area of 50–80 m^2/g. This is to ensure better wettability and better structure of the nanocomposite. All materials were used as received without any further purification.

2.2 Fabrication of nanocomposites

The percentage composition of PLA: GNP is at 95:5 wt% and mixed in the tubular mixer for 6 h to achieve homogeneity of the premixed powder. The percentage weight of 5 wt.% GNP used was based on the findings of Gao et al. [5] where 5 wt.%

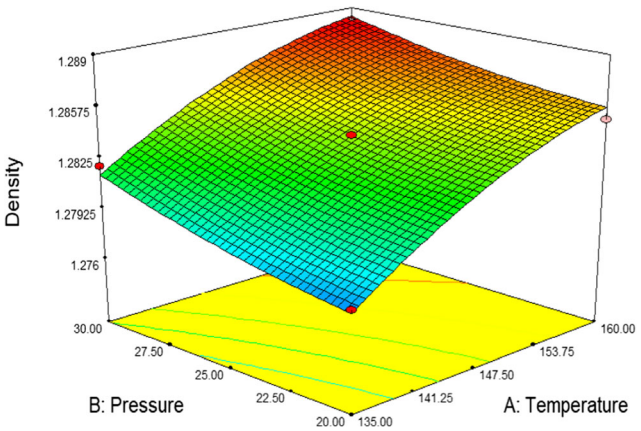

Fig. 3 3-dimensional response surface plot of density as a function of temperature and pressure

Table 4 Actual and predicted response of density

Runs	Factors		Actual	Predicted	Error
	Temperature A (°C)	Pressure B (MPa)	Density (g/cm^3)	Density (g/cm^3)	
1	160.00	30.00	1.288	1.2885	0.0005
2	135.00	30.00	1.282	1.2815	0.0005
3	129.82	25.00	1.276	1.2743	0.0017
4	147.50	17.93	1.283	1.285	0.0020
5	135.00	20.00	1.278	1.2778	0.0002
6	147.50	25.00	1.284	1.284	0.0000
7	147.50	32.07	1.287	1.288	0.0010
8	147.50	25.00	1.284	1.284	0.0000
9	147.50	25.00	1.284	1.284	0.0000
10	147.50	25.00	1.284	1.284	0.0000
11	165.18	25.00	1.288	1.289	0.0010
12	147.50	25.00	1.284	1.284	0.0000
13	160.00	20.00	1.285	1.285	0.0000

GNP inclusion in the PLA matrix gave the best mechanical reinforcement and good dispersion. Agglomeration was observed above this loading level. The 5 μm GNP used in this experiment was observed to give pronounced reinforcing effect due to the large aspect ratio according to the findings of [24, 25]. The pre-mixed powders were weighted in order to obtain a cylinder specimen with 10 mm in thickness and 30 mm in diameter at full densification. The premixed powders were sintered by HPD 25 spark plasma sintering (SPS) machine from FCT Systeme GmbH (Raustein, Germany) at the variation of temperature and pressure. For all the sintering experiments, the heating was from room temperature to the desired temperature at the heating rate of 20 °C/min. At the end of the prescribed holding time of 10 min, applied current was switched off and the sample was rapidly cooled to room temperature. The process was repeated while the other process parameters (temperature and pressure) were varied for different sintered samples.

2.3 Density measurement

The densities of the sintered specimen were determined by the Archimedes method where it involves distilled water as the wetting liquid.

2.4 Hardness measurement

The Vicker micro hardness (HV) at room temperature was used to measure the mechanical properties by a micro hardness tester (Future-tech) at a load (P) of 100 gf (1.0 N) and a dwell time of 15 s. The test results were recorded for each sample with an arithmetic mean of six successful indentations.

2.5 Design of numerical experiment

Design of experiment (DOE) is a statistical technique which determines the significance of each and the interactions with other factors/parameters on the output (responses) of any design [26]. This tool is effective in helping to save the cost incurred in design and manufacturing by reducing numbers of iterations, repetitions, waste, and investigations. It speeds up the process of design and minimizes labour complexity [27, 28].

DOE was set up in this study to understand the influence of SPS processing parameters on the densification and the hardness properties of the polylactic acid/graphene nanocomposite. The statistical analysis and the regression model were generated by using the Design Expert (version 8, State-Ease) based on response surface methodology (RSM) with central composite design (CCD) for process optimization.

SPS process parameters which are temperature (A) and pressure (B) were considered as factors for this study while the densification and hardness were the two experimental

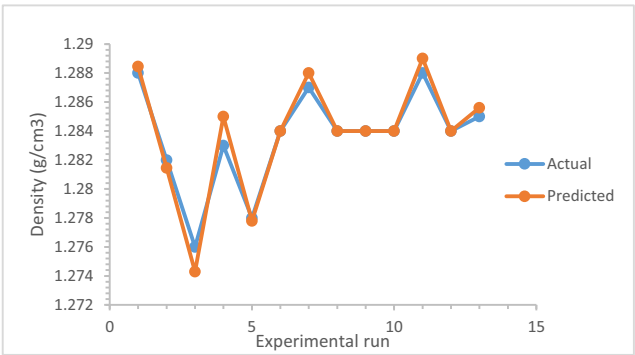

Fig. 4 Actual and predicted values for density

Table 5 Analyses of variance (ANOVA) for response surface quadratic model of hardness of PLA/GNP composite using CCD

Source	Sum of squares	DF	Mean square	*F* value	Prob. > F	
Model	1124.81	5	224.96	174.43	< 0.0001	Significant
A-tempt	1030.60	1	1030.60	799.09	< 0.0001	
B-pressure	65.46	1	65.46	50.75	0.0002	
AB	0.011	1	0.011	8.548×10^{-3}	0.9289	
A^2	24.98	1	24.98	19.37	0.0032	
B^2	1.62	1	1.62	1.26	0.2994	
Residual	9.03	7	1.29			
Lack of fit	9.03	3	3.01			
Pure error	0.000	4	0.0000			
Corr. total	1133.84	12				

R^2 , 0.9920; R^2 ,0.9864; *adequate precision*, 42.373

responses indicated for this study. The DOE approach composed of thirteen (13) experiment called runs using the RSM and CCD.

2.6 The response surface methodology

This is a mathematical and statistical technique used for experimental modeling and analysis of problems in which a response of interest is influenced by several variables and to determine the optimum condition [29]. With response surface methodology (RSM), the functional relationships between the process conditions (temperature and pressure) and the ultimate performance characteristics (density and hardness) of the PLA nanocomposite were determined. The RSM helps to cut-down the numbers of experimental runs to produce a statistically validated result [30]. RSM is well preferred among other experimental design method because it provides a better analysis of the interaction between variables. Moreso, it gives more accurate and complete data with limited numbers of the experiment [31].

This study employs RSM with central composite design (CCD) in investigating the effect of SPS process parameters on the density and hardness property of PLA/GNP nanocomposite. It is aimed at determining the significant parameters that influence the densification and hardness property of the nanocomposite.

The number of experimental runs generated through the RSM can be calculated using Eq. (1)

$$N = 2^{\mathrm{n}} + 2\mathrm{n} + n_{\mathrm{c}} \quad (1)$$

where N is the total number of experiments, n is the number of variables and n_{c} is the number of replicate at the center point. The optimization for PLA/graphene was carried out on these two responses for density and hardness.

2.7 Analysis of variance

The main effect of each factor and interactives effect were determined by carrying out F test (for F and P values) using the statistical tool, analysis of variance (ANOVA) as presented in section 3.2.

3 Experimental result and analysis

The experiment design comprising of a four-level-two factor central composite design model as well as their corresponding responses in terms of density and hardness from the physical experiment is presented in Table 1. The temperature range considered for this experiment is (120–160) °C. The melting temperature as provided in the manufacturer's data sheet is (150–160) °C. Sintering above the melting temperature results in the melting out of the powder out of the die in the SPS chamber. This is in conformity with the working principle of SPS [32]. Sintering at a temperature below this range results in non-consolidation of the admixed powders in the die. The good adhesion between the matrix and the reinforcement

Table 6 Statistical parameters of the model equation as obtained from ANOVA model for hardness

Type of variable	
Standard deviation (SD)	1.14
Mean	250.74
Coefficient of variation CV (%)	0.45
Prediction error sum of square (PRESS)	64.20
R-Squared	0.9920
Adj *R*-squared	0.9864
Predicted *R* squared	0.9434
Adequate precision	42.373

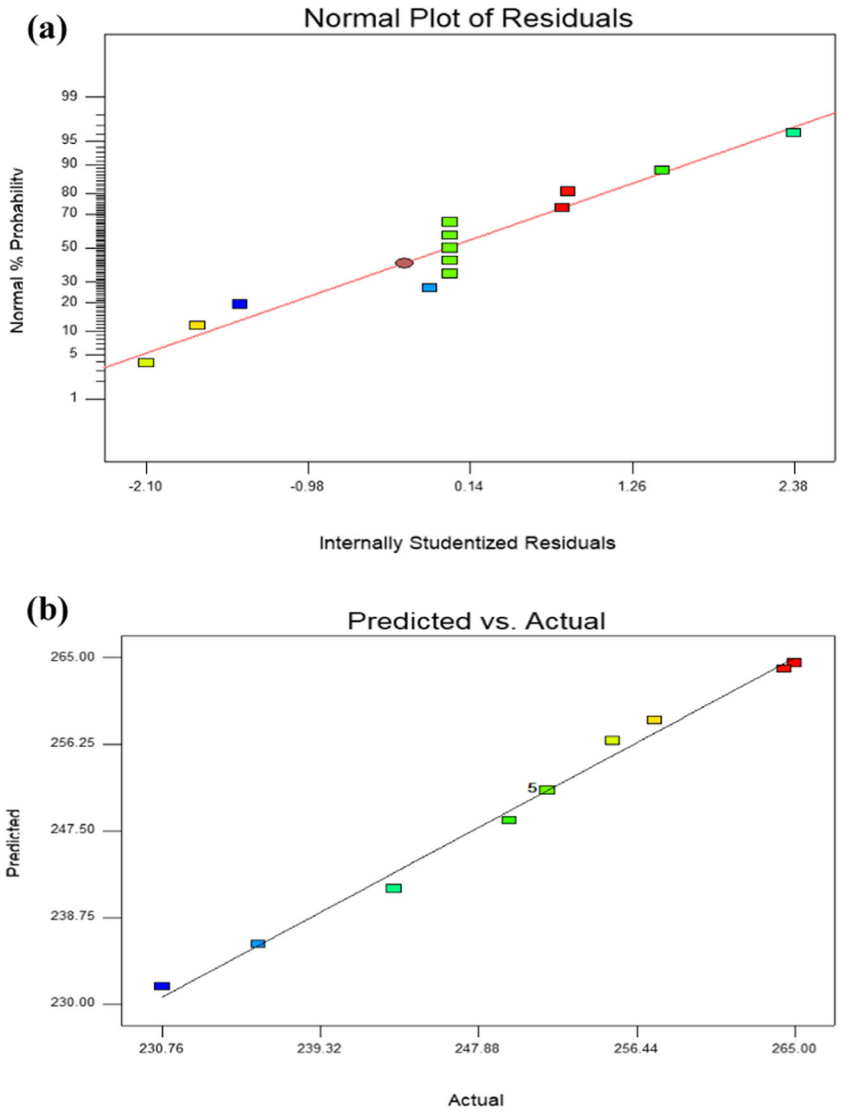

Fig. 5 Stochastic error and a deterministic portion for the hardness of PLA/GNP composites as normal probability plot for residuals (**a**) and predicted versus actual values (**b**)

was influenced by nanoparticle size of the reinforcement. Thereby, resulting in good densification and a high hardness value of the nanocomposite due to minimal porosity.

3.1 Response surface methodology of mechanical properties

The central composite design (CCD) of the response surface methodology (RSM) was employed in determining the levels of factors and the extent of their interaction on the mechanical properties of the graphene-reinforced polylactic acid nanocomposite. The statistical analysis of the results obtained by ANOVA produced a mathematical model that correlates density and hardness as a function of the independent process variables (temperature and pressure). The regression provides the relationship of PLA/GNP composites as a function of temperature and pressure. The test for the significance of the regression model, the significance of individual model coefficient, and the lack of fit are required to determine the adequacy of the model as well as its predictive capability. The test results, as well as the statistical parameters of the model equation as obtained from ANOVA models for density, are presented in Tables 2 and 3 respectively.

3.2 ANOVA analysis and model fitting for density measurement of PLA/GNP composite

From the response surface model for density shown in Table 2, the model F value of 86.10 implies the model is significant. There is only a 0.01% probability that a "model F value" this large could occur due to noise. A very small P value (Prob. > F) indicates that the corresponding coefficient is more significant and so its contribution to the response variable. The value of "Prob. >

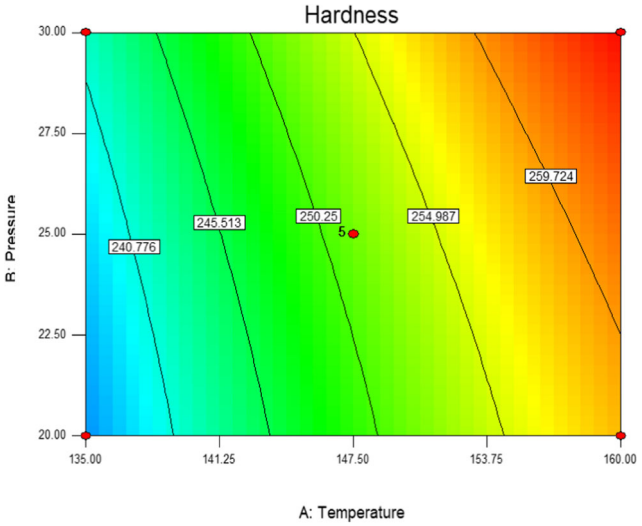

Fig. 6 Plot of hardness as a function of pressure and temperature

F" is less than 0.05 which indicate the significance of the model terms. Values greater than 0.100 indicate the model terms are not significant. The result from the ANOVA for density measurement reveals that three factors terms (A, B, and A^2) are significant model terms and had the largest effect on density at 95% confidence level of significance as indicated by the lowest P value (< 0.05). The P values of other terms are more than 0.05 which implies that their effect on the response model was not statistically significant. The coefficient of determination, R^2 used to measure the reduction of response variability gave (0.9840). This shows that 98.40% of the total variance in the density measurement was attributed to the experimental variables studied. The dispersion is almost totally solved by this model. The closeness of the R^2 value to 1 indicates that the model comprises the best fit of data. Also, the R^2adj. gave 0.9726 which suggest that the model is sufficient without the need for the consideration of additional terms. The standard deviation for the model was 5.758×10^{-4}. The smaller value of standard deviation and the closeness of R^2 value to unity produce a better model giving a predicted value which is closer to the actual value for the response. The difference between the predicted R^2 value of 0.8862 and the adjusted 0.9726 is less than 0.2 showing that they are in reasonable agreement. An adequate precision measures the signal to noise ratio, and a value greater than 4 is desirable. It is computed by dividing the difference between the maximum predicted response and minimum predicted response by the average standard deviation of all the predicted response. A precision value of 30.359 indicates an adequate signal. This model can be used to navigate the design space. The lack of fit test in this study is within the non-significant range relative to pure error which shows that the model fits well with the experimental data.

The quadratic model used to predict the density property of PLA/GNP nanocomposite as a function of temperature (A) and pressure (B) is presented in terms of the coded factors (Eq. 2).

$$\begin{aligned}\text{Density} = {} & +1.28 + 3.746 \times 10^{-3}\,\text{A} + 1.582 \\ & \times 10^{-3}\,\text{B} - 2.5 \times 10^{-4}\,\text{A} - 1.063 \times 10^{-3}\,\text{A}^2 \\ & + 4.375 \times 10^{-4}\,\text{B}^2 \end{aligned} \quad (2)$$

3.3 The normal probability plot of residuals

Residuals are the difference between the respective, observe response, and predicted response. The normal probability plot of residual presents the deviation of actual value against the predicted values. It evaluates the data applied in the model to analyze for the adequacy of the model. A model is said to be adequate if the points on the normal probability plot of the residual forms a straight line. From Fig. 1, the residuals are well aligned on a straight line which implies that the errors are random and the residuals are distributed normally. The closeness of the residual in the prediction of response to the diagonal line implies they are minimal. A weak model always noted by the irregular pattern in the residuals versus the predicted response plots.

3.4 Plots of density measurement

The normal probability plots for residuals and the relationship of the actual versus predicted density are shown in Fig. 1 a, b. The values of R^2 (0.9840) and R^2adj (0.9726) along with the residual analysis adequately fit the model to the experimental data.

Figure 1 a, b show the stochastic error and deterministic portion for the density of PLA/GNP composites for normal

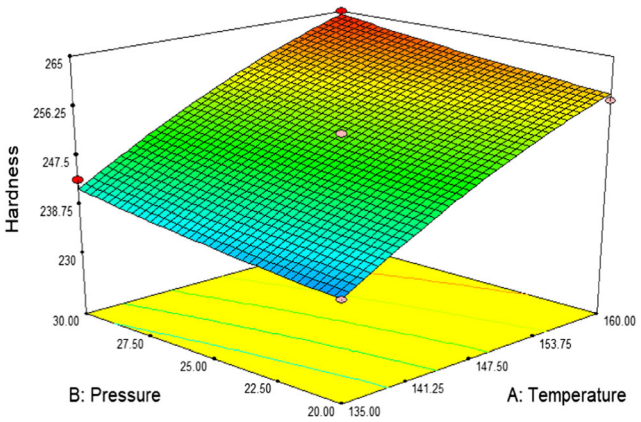

Fig. 7 3D plot of hardness as a function of temperature and pressure.

Table 7 Actual and predicted response of hardness

Runs	Factors		Actual	Predicted	Error
	Temperature A (°C)	Pressure B (MPa)	Hardness (HV)	Hardness (HV)	
1	160.00	30.00	265.00	264.461	0.539
2	135.00	30.00	243.31	241.655	1.655
3	129.82	25.00	230.76	232.38	1.620
4	147.50	17.93	249.55	248.97	0.580
5	135.00	20.00	235.94	236.039	0.099
6	147.50	25.00	251.61	251.61	0.000
7	147.50	32.07	255.16	257.18	2.020
8	147.50	25.00	251.61	251.61	0.000
9	147.50	25.00	251.61	251.61	0.000
10	147.50	25.00	251.61	251.61	0.000
11	165.18	25.00	264.44	266.51	2.070
12	147.50	25.00	251.61	251.61	0.000
13	160.00	20.00	257.42	258.638	1.218

probability plot for residuals as well as the predicted versus actual values respectively. The presence of lack of fit up to six for both figures indicates the adequacy of the model for predictive purpose.

Figures 2 and 3 show the contour as well as the 3D plot for the interactive effects of temperature and pressure on density. From both figures, an increase in temperature and density increases the value of density and vice versa. Small values of temperature and pressure result in a smaller value of density (1.27957 g/cm^3) as indicated by the region in blue color. Increase in temperature and pressure beyond this point results in a significant increase in density up to 1.2848 g/cm^3 as indicated by the region in green color. This region is the most desirable for obtaining the optimum value of density, hence the need to optimization and control temperature and pressure within this region. Further increase in the values of temperature and pressure beyond this region becomes undesirable as indicated by the region in red. This result conforms with that obtained with [33].

The actual and predicted values of density from both the numerical and physical experiment are presented in Table 4.

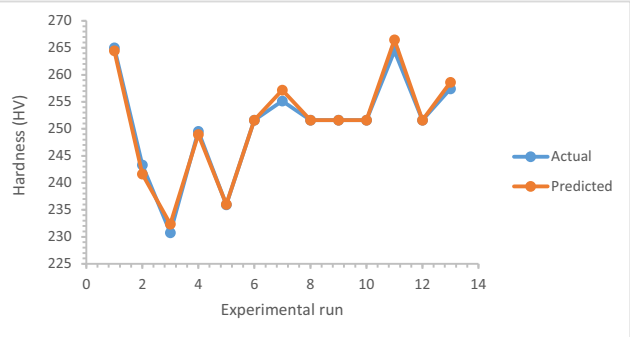

Fig. 8 Actual versus predicted value for hardness

Figure 4 is a plot of the actual values of the density from the physical experiment and the numerical experiment from the developed model.

From Fig. 2, the actual values of density from the physical experiment agree significantly with the predicted values of the developed model with negligible error (Table 4); hence, this confirms that the developed model can adequately predict the values of density.

3.5 ANOVA analysis and model fitting for hardness of PLA/GNP composite

The ANOVA of the RSM for hardness property is presented in Tables 5 and 6. The F value of 174.43 implies the model is significant. There is only a 0.01 chance that a "model F value" this large could occur due to noise. A very small P value (Prob. > F) indicates that the corresponding coefficient is more significant and so its contribution to the response variable values of "Prob. > F" less than 0.500 indicate model terms are significant. Values greater than 0.10 indicate the model is not significant. In this case, A, B, and A^2 are significant for hardness property of the PLA/GNP composite. The lack of fit is said to be insignificant. This is necessary in order to ensure that the developed model fit appropriately. The coefficient of determination, R^2 (0.9920) is very close to 1, in agreement that the model comprises the best data. It shows that 99.2% of the total variance in the density measurement was attributed to the experimental variables studied. The dispersion is almost totally solved by this model. The value of the R^2 adj (0.9864) suggests the model is sufficient without the need for consideration of additional terms. The standard deviation for the model was 1.14. The smaller value of standard deviation and the closeness of R^2 value to unity produce a better model giving a predicted value which is closer to the

Table 8 Optimum combinations of optimization on density and hardness properties of PLA/GNP nanocomposite

Runs	Temperature (°C)	Pressure (MPa)	Density (g/cm^3)	Hardness (HV)
1	158.21	25.87	1.28668	260.465
2	149.01	28.49	1.28573	255.190
3	152.18	25.67	1.28546	255.984
4	153.26	23.79	1.28517	255.774
5	156.66	20.41	1.28526	256.651
6	142.68	25.53	1.28258	247.252
7	158.40	21.65	1.28574	258.336
8	150.57	24.72	1.28477	254.125
9	154.54	22.03	1.28507	255.854
10	150.17	25.47	1.28505	254.720

actual value for the response. The difference between the predicted R^2 value of 0.9434 and the adjusted 0.9864 is less than 0.2; hence, they are in reasonable agreement. Adequate precision measures the signal to noise ratio and a value of greater than 4 is desirable. The adequate precision value of 42.373 indicates adequate signal; hence, the model can be used to navigate space.

The quadratic model used to predict the hardness property of PLA/GNP composites as a function of temperature and pressure is presented in terms of coded factors thus (Eq. 3).

$$\text{Hardness} = +251.61 + 11.35\text{A} + 2.86\text{B} + 0.053\text{AB} - 1.89\text{A}^2 + 0.48\text{B}^2 \quad (3)$$

3.6 The normal probability plot of residuals

The normal probability plots for residuals and the relationship of the actual versus predicted hardness value are shown in Fig. 5a, b. The adequacy of the model is analyzed by evaluating the data applied in the model for hardness. The closeness of the residual in the response prediction to the diagonal line indicates the model is adequate having inherent randomness left over within the error portion. This is good at describing the hardness property. The values of R^2 of 0.9920 and R^2adj 0.9864 along with the residual analysis adequately fit the model to the experimental data.

Figures 6 and 7 show the contour as well as the 3D plot for the interactive effects of temperature and pressure on hardness. From both figures, an increase in temperature and pressure increases the value of hardness and vice versa. Small values of temperature and pressure result in a smaller value of hardness (240.776 HV) as indicated by the region in blue color. Increase in temperature and pressure beyond this point results in a significant increase in hardness value up to 260.00 HV as indicated by the region in green color. This region is the most desirable for obtaining the optimum value of hardness, hence the need to optimize and control temperature and pressure within this region. Further increase in the values of temperature and pressure beyond this region becomes undesirable as indicated by the region in red.

The actual and predicted values of hardness from both the numerical and physical experiment are presented in Table 7.

Figure 8 is a plot of the actual values of the hardness from the physical experiment and the numerical experiment from the developed model.

The actual values of hardness from the physical experiment agree significantly with the predicted values of the developed model with negligible error (Table 7); hence, this confirms that the developed model can adequately predict the values of density.

3.7 Optimization of density and hardness properties

The optimal combination of variables/parameters was carried out by the Design of Expert software. This is to obtain a maximum response that simultaneously satisfied all the variable properties. [34]. From this, thirty (30) optimal solutions/responses were obtained via the optimization process for the process parameters of PLA/GNP nanocomposite. The constraints selected for this study were to be in range. This is to achieve the operating conditions of the SPS technique which requires the operating temperature to be less than the melting point of the material. Else, the material will melt out of the die. The first ten predicted values for each of the response were presented in Table 8. For a given response, the desirability value ranges from 0 to 1. For an ideal case, the value of desirability is one. All the optimal combinations of temperature and pressure on density and hardness properties of the nanocomposite gave a desirability value of one, which implies the case is ideal (Table 8). The number one combination comprising of temperature (158.21 °C), pressure (25.87 MPa), density (1.28668), and hardness (260.465 HV) was selected by the DoE software, although all the combinations indicated the desirability of one. It is clear from the table that solution

number one has the highest values of density and hardness as opposed to others.

4 Conclusions

The influence of SPS processing parameters (temperature and pressure) on the density and hardness properties of the PLA/GNP nanocomposite was studied to obtain optimal performance. The optimal values obtained based on the response surface optimization were the temperature of 158.2 °C and pressure of 25.87 MPa which produced an approximate density of 1.29 and hardness of 260 HV. The marginal differences in the optimized value and experimental trials value validate the reliability of the model. This indicates a negligible error between the optimized and experimental results obtained. Within the range of 135–160 °C, the density was found to increase with pressure irrespective of temperature. Also, the density value was also enhanced with temperature increase at a given pressure. Furthermore, the temperature and pressure also contributed to increasing the hardness value within the given range of temperature and pressure in this study. Hence, both the temperature and pressure have an influence on the density and hardness properties of the nanocomposite. The size of the nanoparticle also played a pivotal role in obtaining better dispersion and good interfacial adhesion between the matrix phase and the reinforcing phase of the nanocomposite. Based on minimal void content, a good density and hardness property were obtained. Optimization is pivotal in obtaining the most feasible combination of the process parameters. The validation of the developed model from RSM and CCD using ANOVA was found to be statistically adequate.

References

1. Halden RU (2010) Plastics and health risks. Annu Rev Public Health 31:179–194
2. Meng Q-K, Heuzey M-C, Carreau P (2012) Effects of a multifunctional polymeric chain extender on the properties of polylactide and polylactide/clay nanocomposites. Int Polym Process 27(5):505–516
3. Kim IH, Jeong YG (2010) Polylactide/exfoliated graphite nanocomposites with enhanced thermal stability, mechanical modulus, and electrical conductivity. J Polym Sci B Polym Phys 48(8):850–858
4. Ahmad E, Luyt A (2012) Morphology, thermal, and dynamic mechanical properties of poly (lactic acid)/sisal whisker nanocomposites. Polym Compos 33(6):1025–1032
5. Gao Y, Picot OT, Bilotti E, Peijs T (2017) Influence of filler size on the properties of poly (lactic acid)(PLA)/graphene nanoplatelet (GNP) nanocomposites. Eur Polym J 86:117–131
6. Singh S, Ghosh AK, Maiti SN, Raha S, Gupta RK, Bhattacharya S (2012) Morphology and rheological behavior of polylactic acid/clay nanocomposites. Polym Eng Sci 52(1):225–232
7. Ayana B, Suin S, Khatua B (2014) Highly exfoliated eco-friendly thermoplastic starch (TPS)/poly (lactic acid)(PLA)/clay nanocomposites using unmodified nanoclay. Carbohydr Polym 110:430–439
8. Chiu WM, Chang YA, Kuo HY, Lin MH, Wen HC (2008) A study of carbon nanotubes/biodegradable plastic polylactic acid composites. J Appl Polym Sci 108(5):3024–3030
9. Li X, Xiao Y, Bergeret A, Longerey M, Che J (2014) Preparation of polylactide/graphene composites from liquid-phase exfoliated graphite sheets. Polym Compos 35(2):396–403
10. Chieng B, Ibrahim N, Yunus WW (2012) Optimization of tensile strength of poly (lactic acid)/graphene nanocomposites using response surface methodology. Polym-Plast Technol Eng 51(8):791–799
11. Sadasivuni KK, Ponnamma D, Thomas S, Grohens Y (2014) Evolution from graphite to graphene elastomer composites. Prog Polym Sci 39(4):749–780
12. Schwertz M, Lemonnier S, Barraud E, Carradò A, Vallat MF, Nardin M (2014) Consolidation by spark plasma sintering of polyimide and polyetheretherketone. J Appl Polym Sci 131(18)
13. Omori M (1994) Functionally gradient materials from Al and polyimide. In: 3rd International Symposium on Structural and Functional Gradient Materials, 1994. Presses polytechniques et universitaires romandes
14. Omori M (1997) Consolidation of thermosetting polyimide by the spark plasma system. J Mater Synth Process 5:279–282
15. Omori M (2000) Sintering, consolidation, reaction and c rystal growth by the spark plasma system (SPS). Mater Sci Eng A 287(2):183–188
16. Omori M, Okubo A, Kang GH, Hirai T (1997) Preparation and properties of polyimide/Cu functionally graded material. In: Functionally graded materials 1996. Elsevier Science BV, pp 767–772
17. Tanaka A, Umeda K, Takatsu S (2004) Friction and wear of diamond-containing polyimide composites in water and air. Wear 257(11):1096–1102
18. Tanaka A, Umeda K, Yudasaka M, Suzuki M, Ohana T, Yumura M, Iijima S (2005) Friction and wear of carbon nanohorn-containing polyimide composites. Tribol Lett 19(2):135–142
19. Sébileau JC, Lemonnier S, Barraud E, Vallat MF, Carradò A, Nardin M (2017) Consolidation by spark plasma sintering (SPS) of polyetheretherketone. J Appl Polym Sci 134(23)
20. Ge ZH, Chang Y, Li F, Luo J, Fan P (2018) Improved thermoelectric properties of PEDOT: PSS polymer bulk prepared using spark plasma sintering. Chem Commun 54(19):2429–2431
21. Tharazi I, Sulong AB, Muhamad N, Haron CHC, Tholibon D, Ismail NF, Radzi MKFM, Razak Z (2017) Optimization of hot press parameters on tensile strength for unidirectional long kenaf fiber reinforced polylactic-acid composite. Procedia Eng 184:478–485
22. Shaari A, Seman MA, Faizal C (2017) Optimization of mechanical properties of silver nanoparticles (AgNPS)-loaded chitosan/polylactic acid (PLA) biofilms by using response surface methodology (RSM). in MATEC Web of Conferences. EDP Sciences
23. Ibrahim N, Jollands M, Parthasarathy R (2017) Optimizing processing conditions of PLA nanocomposites using response surface methodology. Pertanika J Sci Technol 25(S):63–72
24. Wang F, Drzal LT, Qin Y, Huang Z (2015) Mechanical properties and thermal conductivity of graphene nanoplatelet/epoxy composites. J Mater Sci 50(3):1082–1093
25. Wang F, Drzal LT, Qin Y, Huang Z (2016) Size effect of graphene nanoplatelets on the morphology and mechanical behaviour of glass fiber/epoxy composites. J Mater Sci 51(7):3337–3348

26. Lundstedt T, Seifert E, Abramo L, Thelin B, Nyström Å, Pettersen J, Bergman R (1998) Experimental design and optimization. Chemom Intell Lab Syst 42(1–2):3–40
27. Mehat NM, Kamaruddin S (2011) Multi-response optimization of injection moulding processing parameters using the Taguchi method. Polym-Plast Technol Eng 50(15):1519–1526
28. Lee KS, Jeon B, Cha SW, Jeong KY, Han IS, Lee YS, Lee K, Cho SM (2011) A study on optimizing the mechanical properties of glass fiber-reinforced polypropylene for automotive parts. Polym-Plast Technol Eng 50(1):95–101
29. Baş D, Boyacı IH (2007) Modeling and optimization I: usability of response surface methodology. J Food Eng 78(3):836–845
30. Ghasemi I, Karrabi M, Mohammadi M, Azizi H (2010) Evaluating the effect of processing conditions and organoclay content on the properties of styrene-butadiene rubber/organoclay nanocomposites by response surface methodology. Express Polym Lett 4(2):62–70
31. Chow W, Yap Y (2008) Optimization of process variables on flexural properties of epoxy/organo-montmorillonite nanocomposite by response surface methodology. Express Polym Lett 2:2–11
32. Babalola BJ, Shongwe MB, Obadele BA, Olubambi PA (2018) Densification, microstructure and mechanical properties of spark plasma sintered Ni-17% Cr binary alloys. Int J Adv Manuf Technol:1–9
33. Schwertz M, Ranque P, Lemonnier S, Barraud E, Carrado A, Vallat MF, Nardin M (2015) Optimization of the spark plasma sintering processing parameters affecting the properties of polyimide. J Appl Polym Sci 132(9)
34. Safizadeh MH, Thornton BM (1984) Optimization in simulation experiments using response surface methodology. Comput Ind Eng 8(1):11–27